Aleksandar M. Milovanović[1], Igor Martić[2], Ljiljana Trumbulović[1], Ljubica Diković[1], Branko Drndarević[3]*

FINITE ELEMENT ANALYSIS OF SPHERICAL STORAGE TANK STRESS STATE

ANALIZA NAPONSKOG STANJA SFERNOG REZERVOARA METODOM KONAČNIH ELEMENATA

Originalni naučni rad / Original scientific paper
UDK /UDC:

Rad primljen / Paper received: 30.11.2021

Adresa autora / Author's address:
1) Western Serbia Academy of Applied Studies, Užice, Serbia email: aleksandar.milovanovic@vpts.edu.rs
2) University of Belgrade, Innovation Centre of the Faculty of Mechanical Engineering, Belgrade, Serbia
3) Rad-Raso d.o.o., Užice, Serbia

Keywords
- finite element analysis (FEA)
- pressure vessel
- spherical storage tank

Ključne reči
- metoda konačnih elemenata
- oprema pod pritiskom
- sferni rezervoar

Abstract

In this paper, a spherical storage tank for the storage of liquefied petroleum gas is analysed. A design calculation of structural elements is performed according to valid standards and technical regulations. Seismic loads are determined. By using the finite element method, a structural analysis of the spherical storage tank is performed for the design case in which the storage tank is exposed to effects of: self-weight of sphere with supporting pillars; complete reinforcement; staircases and platforms; snow; hydrostatic pressure of the working fluid; design pressure; and horizontal seismic forces. The zones with maximum stress values are shown and the obtained results are analysed.

Izvod

U radu je za analizirani sferni rezervoar za skladištenje tečnog naftnog gasa urađen kontrolni proračun elemenata konstrukcije prema važećim standardima i tehničkim regulativima. Određena su opterećenja od dejstva seizmike. Primenom metode konačnih elemenata urađena je strukturna analiza konstrukcije sfernog rezervoara za proračunski slučaj u kome je rezervoar izložen dejstvu: sopstvene težine sfere sa stubovima; kompletnom armaturom; stepenicima i platformama; težine snega; hidrostatičkog pritiska radnog fluida; proračunskog pritiska; i horizontalne seizmičke sile. Prikazane su zone sa maksimalnim vrednostima napona i izvršena je analiza dobijenih rezultata.

INTRODUCTION

The paper analyses the spherical storage tank for liquefied petroleum gas with an outside diameter D_e = 12 263.0 mm, volume V = 950 000 l, exposed to the effect of the internal design pressure p = 16.7 bar. The design temperature is 40°C. The spherical casing of the storage tank is made of A516 Gr 70 /1/, the supporting pillars (tubular legs) are made of material A283 Gr C /1/, the bracings of the supporting pillars are made of A194 2N /1/, the flanges of the pipe fittings of the spherical storage tank are made of material A105 /1/. The allowable stress of the spherical storage tank elements is determined according to standard EN 13445-3: 2021, /2/, according to the following expression:

$$f = \min\left(\frac{R_m}{2.4}, \frac{R_{p0.2t}}{1.5}\right). \qquad (1)$$

Allowable stress for storage tank elements of material A516 Gr 70 (ASTM):
- spherical shell, main stresses f = 173.33 N/mm^2, ($R_{p0.2t}$ = 260 N/mm^2; R_m = 485 N/mm^2);
- spherical shell, local stresses f_l = 260 N/mm^2.

Allowable stress for storage tank elements of material A283 Gr C (ASTM):
- supporting pillar, local stresses f_l = 205 N/mm^2, ($R_{p0.2t}$ = 205 N/mm^2; R_m = 380 N/mm^2).

Allowable stress for storage tank elements of material A194 2N (ASTM):
- bracings of the supporting pillar, main stresses f = 166.67 N/mm^2.

Allowable stress for storage tank elements of material A105 (ASTM):
- pipe fitting flanges, main stresses f = 166.67 N/mm^2, ($R_{p0.2t}$ = 250 N/mm^2; R_m = 485 N/mm^2).

DESIGN CALCULATION

Calculation of the required wall thickness of spherical storage tank casing, for the storage of liquefied petroleum gas, according to standard EN 13445-3: 2021, /2/:
p = 16.7 bar - design pressure,
D_e = 12263 mm - outside diameter of the shell,
D_i = 12197 mm - inside diameter of the shell,
z = 1 - coefficient of the welded joint,
c = 1 mm - corrosion allowance.

Required wall thickness of the spherical shell:

$$e_p = \max\left(\frac{D_e p}{4fz + p} + C;\ \frac{D_i p}{4fz - p} + C\right) = 30.47 \text{ mm}. \qquad (2)$$

The nominal wall thickness of the spherical shell of the spherical storage tank for the storage of liquefied petroleum gas is e_n = 33 mm.

Seismic load calculation according to technical regulations on wind effects on supporting steel structures, /3/:
- input data (object category I):

K_0 = 1.5 - object category coefficient,

K_s = 0.1 - seismic intensity coefficient (IX degree according to MCS scale),
K_d = 1.0 - coefficient of the dynamics,
K_p = 1.0 - coefficient determined by damping and ductility of the structure,
G = 1884 kN - total self-weight of the object, equipment, and useful loads,
G_{rm} = 9682 kN - load from working matter.

Determination of total horizontal seismic force:
$K = K_0K_sK_dK_p$ = 0.15 - total seismic coefficient for horizontal direction,
$G_r = G + G_{rm}$ = 11565 kN - total vertical load in operation,
$S = KG_r$ = 1735 kN - total horizontal seismic force.

Determination of total vertical seismic force:
$K_p = 0.7K_0K_sK_dK_p$ = 0.105 - total seismic coefficient for the vertical direction,
$S_v = K_vG_r$ = 1214 kN - total vertical seismic force.

FINITE ELEMENT MODEL OF THE SPHERICAL STORAGE TANK STRUCTURE

In order to form a finite element model of the spherical storage tank structure with a completely realistic geometric shape, it is necessary to draw all its structural details in 3D form, based on the original documentation provided by the client, Fig. 1. When modelling a spherical storage tank, the basic structural elements are the shell, supporting pillars, and bracings.

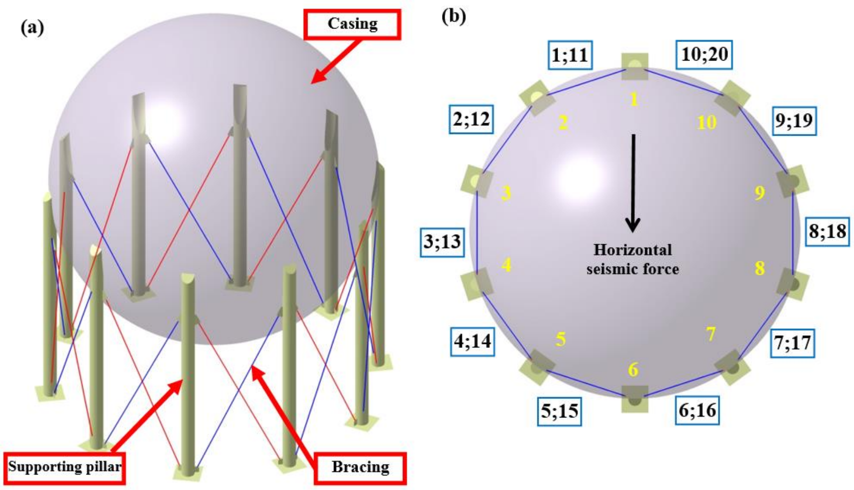

Figure 1. Spherical storage tank (first group of bracings from 1 to 10 are shown in red, while the second group from 11 to 20 are shown in blue): a) isometric view; b) top view.

The support of the spherical storage tank is performed using 10 radially arranged pillars whose numbering is shown in yellow numbers in Fig. 10b. The supporting pillars are connected by two groups of 10 bracings each. The first group of bracings is shown in red in Fig. 1a, while the second group of bracings is shown in blue. The numbering of the bracings in Fig. 1b is performed in the positive mathematical direction, and the numeration is encircled in blue. The horizontal seismic force, whose influence on the stress-strain state of the structure is analysed in the second section of this paper and has served as a reference point for the numbering of structural elements.

By synthesizing the presented elements, a 3D model of a spherical storage tank is formed. It represents a continuum for the formation of the finite element model, /4/.

Details of the finite element mesh generated in the zones of connection of the supporting pillars and the shell of the spherical storage tank and the connection of the pillar, pillar base, reinforcing plates, and bracings is shown in Fig. 2.

The support of the model is achieved by preventing all degrees of freedom by the support base of the pillar.

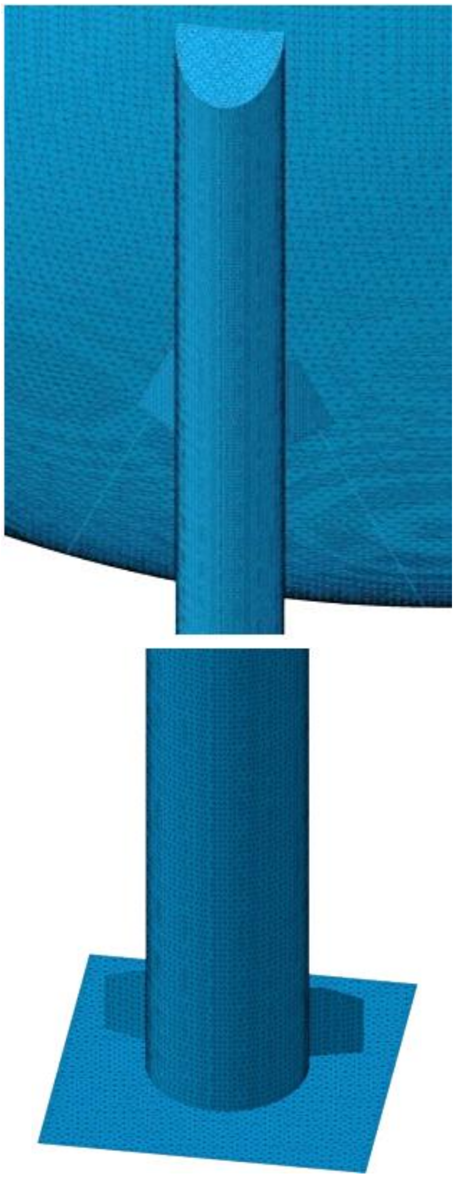

Figure 2. Details of the finite element mesh: (left) connection zone of the supporting pillar and the shell of the spherical storage tank; (right) pillar support zone

The finite element mesh consists of 1315748 triangular elements of the plate type and 7160 finite elements of the beam type, which contain a total of 674110 nodes. The connection of the corresponding structural elements is performed with the help of 9308 virtual beam elements, which simulate the connection of structural elements by welding. The total number of degrees of freedom in the system in this case is 4023120.

The solution of this system by displacements is not possible due to the singularity of the global stiffness matrix (det[k] = 0), because the structures do not eliminate displacements in space (three translations and three rotations), so the system cannot be deformed due to the given load. By reducing the system for given displacements, i.e. for 160836 equations in the place of supports, the number of nonhomogeneous linear algebraic equations of the system is obtained, which in this case is 3862257.

In matrix form, the system of equations reads /5/:

$$\{F\}=[\mathrm{k}]\{\Delta\}\rightarrow\begin{Bmatrix}F_S\\F_R\end{Bmatrix}=\begin{bmatrix}K_{SS} & K_{SR}\\K_{RS} & K_{SS}\end{bmatrix}\begin{Bmatrix}\Delta_S\\\Delta_R\end{Bmatrix}. \quad (3)$$

Since the displacement vector is in the places of supports,

$$\{\Delta_R\}=\{0\}, \quad (4)$$

unknown nodal displacements are obtained from the matrix equation,

$$\{\Delta_S\}=[K_{ss}]^{-1}\{F_S\}, \quad (5)$$

in which: $\{\Delta_S\}$ - vector of unknown displacements of each node of the finite element mesh; $\{F_S\}$- a given load vector; $[K_{SS}]$ - submatrix of the global stiffness matrix of a finite element mesh system.

Determining the field by moving the model, the system is statically identified. By use of equations of displacement and deformation, as well as equations of deformation and stress, the stress state of the model is determined, /5/.

The deformation vector is obtained according to the matrix equation,

$$\{\varepsilon\}=[\mathrm{B}]\{\Delta\}=\begin{bmatrix}\mathrm{B}_i & \mathrm{B}_j & \mathrm{B}_k\end{bmatrix}\{\Delta_S\}. \quad (6)$$

The stress vector is calculated based on expression,

$$\{\sigma\}=[\mathrm{D}]\{\varepsilon\}=[\mathrm{D}]\begin{bmatrix}\mathrm{B}_i & \mathrm{B}_j & \mathrm{B}_k\end{bmatrix}\{\Delta_S\}. \quad (7)$$

LOAD ANALYSIS

Structural analysis /4/ of the spherical storage tank is performed for the design case in which the structure of the spherical storage tank is exposed to the effects of:

- self-weight of the sphere with pillars, complete reinforcement, staircases, and platforms (Q = 1884 kN);
- snow weight (Q_S = 34.7 kN);
- hydrostatic pressure of the working fluid (distribution along the contour of the sphere is shown in Fig. 3);
- design pressure (p = 16.7 bar);
- horizontal seismic forces (S = 1735 kN).

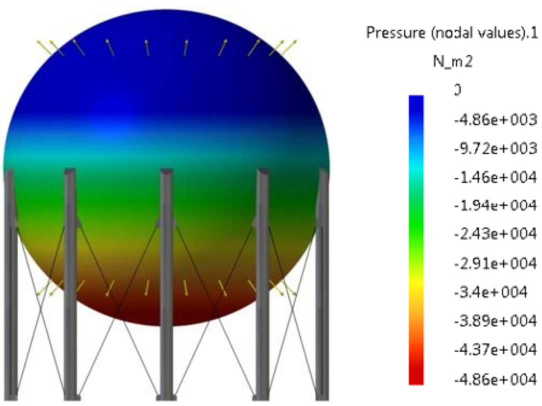

Figure 3. Hydrostatic pressure field of the working fluid.

The horizontal seismic force is introduced into the model as a continuous load of one spherical cap of the spherical storage tank shell, the resultant of which is in the centre of gravity of the sphere structure, Fig. 4.

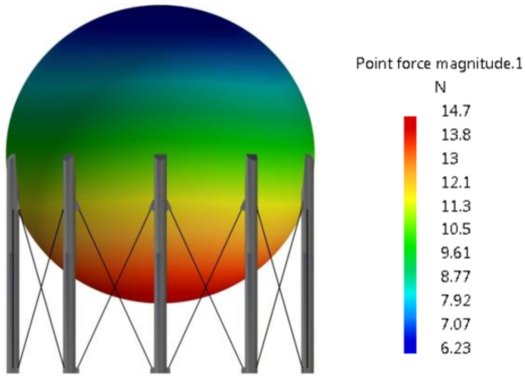

Figure 4. Nodal loads due to horizontal seismic force.

The design pressure in the models is entered as a uniform pressure field acting on the surface of the sphere shell, while the self-weight of the structure is simulated by introducing the acceleration of the Earth's gravity to all nodes of the finite element mesh.

STRESS STATE OF SPHERICAL STORAGE TANK STRUCTURE

Stress state of the spherical storage tank is performed for the design loads. This is done using von Mises hypothesis for stress /5-12/:

$$\sigma_u=\sqrt{\frac{1}{2}\left[(\sigma_x-\sigma_y)^2+(\sigma_y-\sigma_z)^2+(\sigma_z-\sigma_x)^2\right]+3(\tau_{xy}^2+\tau_{yz}^2+\tau_{zx}^2)} \quad (8)$$

Uniaxial stress is suitable for deriving stress evidence because it is compared with tabular data (obtained by uniaxial tightening of test tubes) for the applied material. Stress values shown in stress field images are in MPa.

Table 1. Dependence of stress (MPa) in the shell on height (m) of the working fluid column.

height	0	1	2	3	4	5	6
Stress	154.5	154.5	154.5	154.5	154.8	155.3	155.9
Height	7	8	9	10	11	12	12.23
Stress	156.4	157.0	157.5	158.0	158.6	159.1	159.2

Figure 5b shows a diagram of spherical storage tank shell stress dependence on the height of working fluid column, while Table 1 shows increase in stress with increasing height of fluid column with one meter step. While acquiring data for this diagram, care is taken to avoid stress jumps and values that inevitably occur in zones of connection of supporting pillars and shell of the spherical storage tank.

When modelling the joints of supporting pillars, a very conservative approach is applied, namely the models do not include welded joints that would significantly contribute to increase in thickness of ligaments at the joints, thus obtaining a pronounced stress concentration in the observed zones.

Maximum stress values in zones of the joints of supporting pillars and the shell of spherical storage tank are given in Table 2, while stress fields in zones of connections of the pillars and casing are shown in Fig. 6.

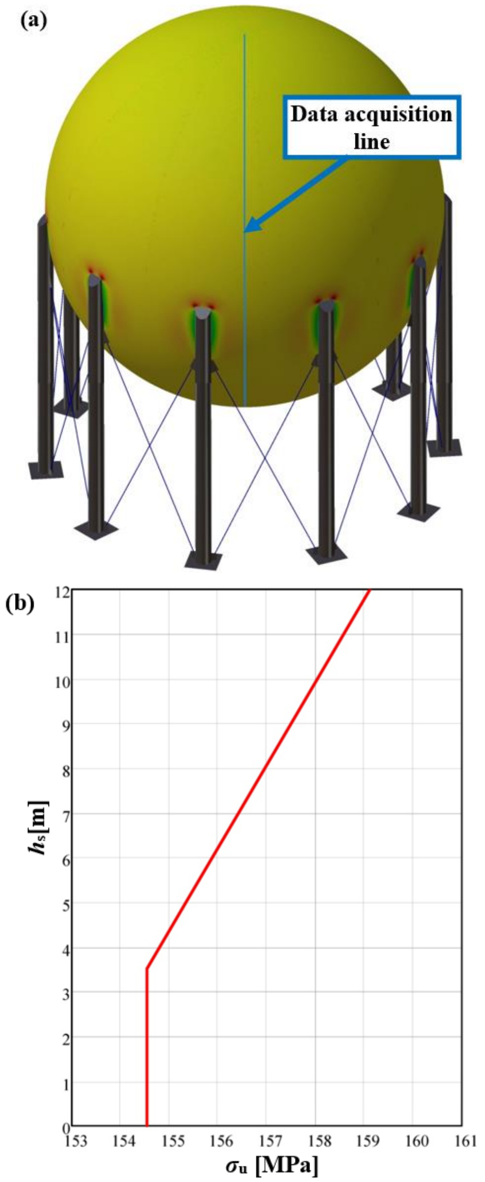

Figure 5. Stress distribution in spherical storage tank casing with increase in height of the working fluid column.

Table 2. Maximum stresses in joint zones of pillars and shell.

Pillar zone	1	2	3	4	5
Maximum stress [MPa]	176	190	214	224	226
Pillar zone	6	7	8	9	10
Maximum stress [MPa]	216	227	225	214	190

The maximum comparative stress occurs in the zone of connection with pillar 7 and is $\sigma_{max,s}$ = 227 MPa. This design case is relevant for examining the load capacity of supporting pillars and bracings of the spherical storage tank. The maximum values of comparative stresses that occur in supporting pillars are shown in Fig. 7. For easier visual identification in Fig. 7, the numbering of the pillars is performed in accordance with recommendations given in Fig. 1. The maximum comparative stress occurs in pillar 7 in the zone of connection of the sphere shell and pillar structure, and is $\sigma_{max,s}$ = 206 MPa.

Stress fields in bracings of the first and second groups are shown in Figs. 8-9, while maximum stress values that occur in bracings are given in Tables 3-4.

Results shown in Tables 3-4 indicate linear correlation of maximum stress values that occur in bracings of the first and second group. Namely, the maximal value of comparative stress of 102 MPa occurs in the third bracing from the first group. This value fully corresponds to the stress value that occurs in the symmetrically placed bracing 18 of the second group. The same is the case with the second group of bracings i.e. bracings 4 from the first group and 17 from the second group whose maximum stresses are 87 MPa.

Table 3. Maximum stresses in bracings 1 to 10.

Bracing	1	2	3	4	5
Maximum stress (MPa)	31	80	102	87	44
Bracing	6	7	8	9	10
Maximum stress (MPa)	14	63	85	71	27

Table 4. Maximum stresses in bracings 11 to 20.

Bracing	11	12	13	14	15
Maximum stress [MPa]	27	71	85	63	14
Bracing	16	17	18	19	20
Maximum stress [MPa]	44	87	102	80	31

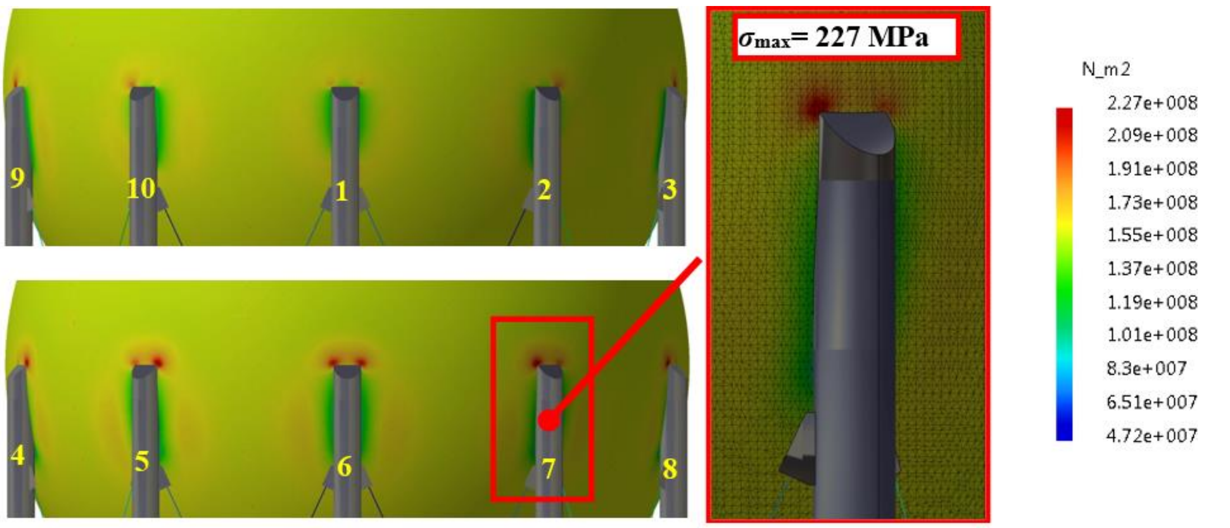

Figure 6. Stress field in joint zones of pillars and spherical storage tank shell (pillars are numbered according to markings in Fig. 1b).

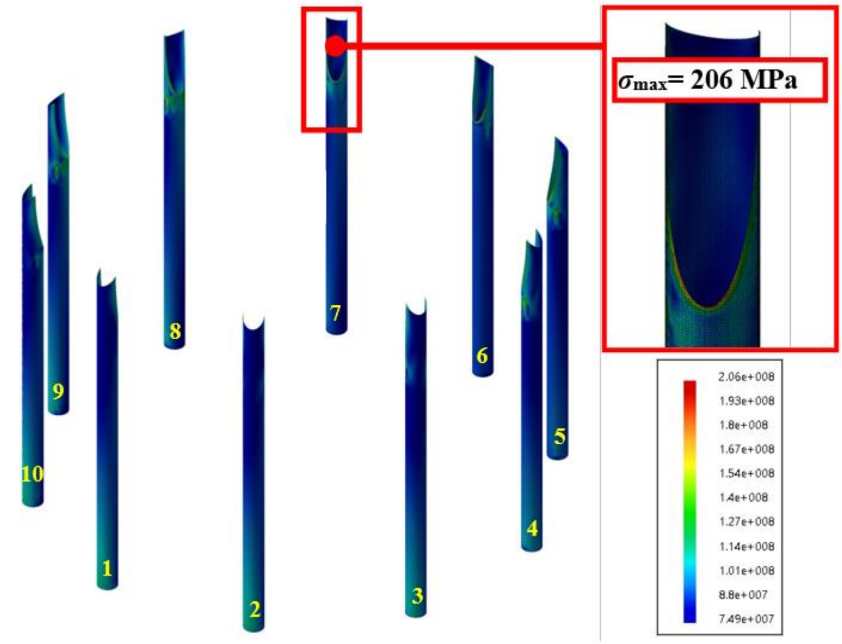

Column	σ_{max} [MPa]
1	192
2	176
3	182
4	182
5	204
6	182
7	**206**
8	187
9	185
10	172

Figure 7. Stress field of spherical storage tank support pillars.

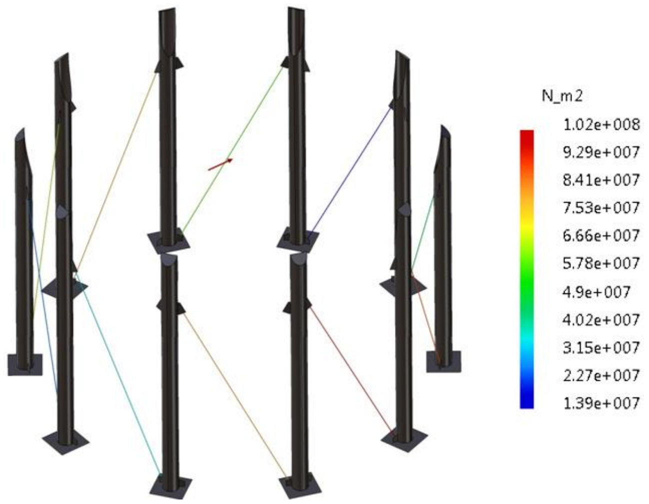

Figure 8. Stress field in bracings 1 to 10.

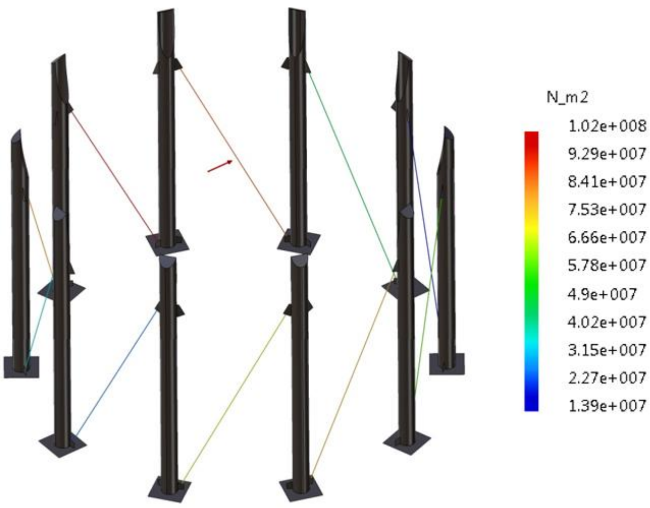

Figure 9. Stress field in bracings 11-20.

DISCUSSION

Maximum stresses - allowable stresses

Table 5 shows maximum stresses values obtained due to the effect of combined load (effects of self-weight of sphere with pillars, complete reinforcement, staircases and platforms; snow weight; hydrostatic pressure of the working fluid; designed pressure; horizontal seismic force). The maximum comparative stress that occurs in the spherical shell is 159.2 MPa, the maximum local stress in the spherical shell is 227 MPa, the maximum local stress in the joint of the supporting pillar and spherical shell is 206 MPa, and the maximum comparative stress in the supporting pillars is 102 MPa.

Table 5. Maximum stress values obtained due to the effect of combined loading.

load case	main stresses in spherical shell		local stresses: sphere		local stresses: pillars		bracings: I group	bracings: II group	bracings
	Max. stress (MPa)								
(p_r, p_h, S, m_{s+r})	159	173.3 S = 1.5	227	260 S = 1	206	260 S = 1	102	102	166.67 S = 1.5

CONCLUSIONS

The analysed spherical tank for storing liquefied petroleum gas, volume V = 950 000 l, outside diameter D_e = 12 263 mm, is constructed with existing standards and regulations for pressure equipment. The calculation according to standard EN 13445-3: 2021 determines the minimum required wall thickness of spherical storage tank elements, based on which the adopted nominal value is determined. According to technical documentation, a 3D model of the spherical storage tank is created, based on which a finite element model is formed that is exposed to certain effects of:

– self-weight of sphere with pillars, complete reinforcement, staircases, and platforms; (Q = 1884 kN);

– snow weights (Q_S = 34.7 kN);
– hydrostatic pressure of working fluid;
– design pressure (p = 16.7 bar);
– horizontal seismic forces (S = 1735 kN).

By analysing the results obtained by applying scientifically verified finite element method, the zones with highest stresses are determined. These zones are additionally analysed in order to determine their influence on the integrity of the spherical storage tank structure. The main comparative stress value in the spherical shell, f_u = 159.2 MPa, is lower than the allowable stress value for the spherical shell, f = 173.3 MPa. The local stress value in the analysed zones of the spherical shell, f = 227 MPa, is lower than local allowable stress, f_l = 260 MPa. The local stress value in the welded joint of the support pillar and spherical shell, f = 206 MPa, is lower than the local allowable stress, f_l = 260 MPa. The comparative stress value in the bracings, f_u = 102 MPa, is lower than the allowable stress, f = 166.67 MPa. By comparing maximum comparative stresses and allowable stresses, it can be concluded that the integrity of the spherical storage tank structure exposed to combined loading will not be compromised, since the values of maximal stresses reach: 91.8 % of allowable stress for spherical shell; 87.3 % of allowable stress for spherical shell in the local zone; 79.2 % of allowable stress in the local zone of welded joint of supporting pillars and spherical shell; 61.2 % of allowable stress for bracings of the supporting pillars.

REFERENCES

1. ASME/ASTM, standard on material properties and testing.
2. EN 13445-3: 2021, Unfired pressure vessels. 2021.
3. AD2000, Technical Rules for Pressure Vessels, 2003, p.707.
4. Zamani, N.G., CATIA V5 FEA Tutorials Release 20, SDC Publications, 2011.
5. Bathe, K.J., Finite Element Procedures, 2nd Ed., Watertown, MA, USA, 2016.
6. Đurđević, Đ., Đurđević, A., Anđelić, N., Petrović, A. (2021), *Numerical-experimental determination of stress and deformation state in connection lugs*, Struct. Integ. and Life 21(2): 169-172.
7. Đurđević, Đ., Sedmak, S., Đurđević, A., et al. (2021), *Development and calculation of supporting structure for mining power equipment*, Struct. Integ. and Life, 21(2): 173-177.
8. Radojković, M., Čamagić, I., Šarkočević, Ž., et al. (2021), *Stress distribution on an isotropic plate with a rectangular opening under biaxial tension load*, Struct. Integ. and Life 21(1): 91-94.
9. Sandić, U., Tomić, R., Grbović, A., Sedmak, A. (2020), *Failure analysis of bicycle frame composite structure based on stacking variant of laminate layers*, Struct. Integ. and Life, 20(1): 69-76.
10. Mijatović, T., Milovanović, A., Sedmak, A., et al. (2019), *Integrity assessment of reverse engineered Ti-6Al-4V ELI total hip replacement implant*, Struct. Integ. and Life, 19(3): 237-242.
11. Đurđević, Đ., Anđelić, N., Milošević-Mitić, V., et al. (2019), *Influence of encastering on thin-walled cantilever beams with U and Z profiles on the magnitude of equivalent stress and deformation*, Struct. Integ. and Life, 19(3): 251-254.
12. Maksimović, S., Maksimović, M., Maksimović, K., et al. (2019), *Numerical and experimental stress analysis of layered composite structures subject to mechanical and hygrothermal loads*, Struct. Integ. and Life, 19(1): 45-49.